

The advanced prediction of threshold stress for hydride reorientation in Zircaloy-4 cladding tube based on thermodynamic model and EBSD analysis

Dongyeon Kim, Youho Lee*

Seoul National University, Gwanak-ro 1, Gwanak-gu, Seoul 08826, Republic of Korea

*Corresponding author: leeyouho@snu.ac.kr

1. Introduction

Zirconium-based alloy is used as material of nuclear fuel cladding. In reactor, hydrogen is absorbed into the cladding and precipitates in circumferential hydride form. Circumferential hydride reorients in radial direction under hoop stress above threshold. Hydride reorientation in the cladding is a major degradation mechanism of spent nuclear fuel in dry storage, because radial hydrides are susceptible to mechanical stress, and then can cause fracture of cladding tube which has a role as secondary radiation protection boundary.

Many studies to analyze and predict threshold stress of hydride reorientation have been conducted by means of both mechanical experiments and theoretical prediction with thermodynamic models. However, a gap between experimental results (65~138 MPa) and theoretical predictions exists beyond understandable range [1-4]. In order to reduce this gap and increase accuracy of prediction, (1) texture of α -zirconium (α -Zr) matrix (HCP structure) in the cladding and (2) average fraction of Zr-hydride interface orientation relationships were analyzed from information obtained by EBSD (Electron Backscatter Diffraction) in this study. The developed thermodynamic model and the more accurate prediction of hydride reorientation threshold stress will improve our understanding on hydride reorientation and help us contrive prevention designs from it.

2. Experimental setup

As-received commercial Zircaloy-4 cladding tube was used as specimens (inner and outer diameters are 8.36 mm and 9.5 mm, respectively, and its nominal chemical composition is Zr-1.5w%Sn-0.2w%Fe-0.1w%Cr). They were charged with hydrogen in a vacuum furnace (see Fig. 1) at 400 °C to replicate discharged spent nuclear fuels from nuclear reactor.

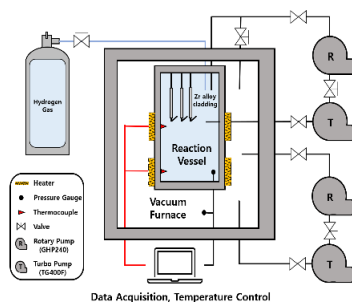


Fig. 1. Schematic illustration of hydrogen charging facility

In order to induce hydride reorientation in Zr matrix of cladding, hydride reorientation treatment was conducted by simulating the dry storage environment with an experimental facility as shown in Fig. 2. A 5 mm hydrogenated specimen was located in tensile jigs of tensile test system (INSTRON 8616) and heated from 20 °C to 400 °C for 2 hours. After the stabilization time for 1 hour at 400 °C, a constant tensile load was applied to the specimen throughout the cooling time for 10 hours to make radial δ -hydrides (FCC structure). Optical microscope (Nikon EPIPHOT 300), FE-SEM (JEOL JSM-7900F Schottky gun type) and EBSD (Oxford instruments Symmetry CMOS type) were utilized to characterize microstructure of five radial hydride areas. For the detailed analysis on microstructure, EBSD images were post-processed with OIM analysis software (EDAX OIM Analysis ver.8). The concentrations of hydrogen in each specimen were measured as 458.2 ± 42.6 wppm by using a hot vacuum extraction mass spectroscopy (ELTRA ONH-2000).

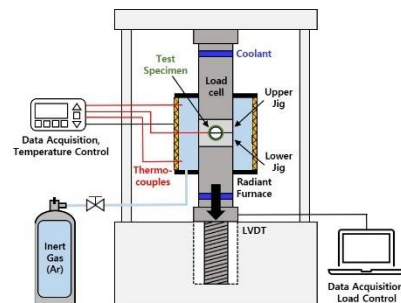


Fig. 2. Schematic illustration of hydrogen reorientation treatment facility

3. Thermodynamic model for theoretical prediction of hydride reorientation

Among many theoretical analysis on hydride reorientation, it is known that the thermodynamic model developed by W. Qin et al. [5,6] is the most advanced. According to them, the Gibbs free energy of radial hydride nucleation (Eq. (1)) consists of chemical free energy, strain energy, interaction energy, interface energy and grain boundary energy. From it, the critical nucleation energy (ΔG_{\perp}^*) of δ -hydride under tensile stress can be expressed in the following Eq. (2) [5].

$$\Delta G = -V(\Delta G_{chem} + Pv) + A\Delta G_{interface} + V\Delta G_{strain} - S\Delta G_{GB} - V\Delta G_{interaction} \quad (1)$$

$$\Delta G_{\perp}^* = \frac{Z}{[-\Delta G_{chem} - \left(\frac{x}{\bar{v}_{hyd}}\right)\left(\frac{\sigma_{\theta} \cos \phi}{3}\right)\bar{v}_H - \sigma_{\theta} \cos \phi \chi + \Delta G_{strain}]^2} \quad (2)$$

where Z is $18\pi\gamma_{\alpha\delta}^c\gamma_{\alpha\delta}^2$ for an intragranular hydride or $(16\pi/3)\gamma_{\alpha\delta}^3f$ for an intergranular hydride ($\gamma_{\alpha\delta}$ is the disordered interfacial energy, $\gamma_{\alpha\delta}^c$ is the coherent interfacial energy, f is the δ -hydride's shaping factor), ΔG_{chem} is the chemical free energy absolute value of transformation per unit volume, ΔG_{strain} is the strain energy per unit volume of the δ -hydride, χ is the α -Zr matrix- δ -hydride misfit strain, \bar{v}_{hyd} and \bar{v}_H are the molar volumes of the hydrides and hydrogen in the α -Zr matrix, respectively, x is the ZrH x composition ratio, σ_{θ} is the applied hoop stress, and ϕ is the angle between the hoop stress (σ_{θ}) and the normal to hydride plane (n_{hyd}). The denominator of **Eq. (2)** is composed of the driving force for radial hydride nucleation, $-\Delta G_{chem} - (x/\bar{v}_{hyd})(\sigma_{\theta} \cos \phi/3)\bar{v}_H - \sigma_{\theta} \cos \phi \chi$ and the resistant force, ΔG_{strain} . For the formation of radial hydride under applied stress, the driving force should be larger than the resistant force. Therefore, a criterion of hydride reorientation can be expressed in **Eq. (3)** and then threshold hoop stress can be calculated with **Eq. (4)** by manipulating **Eq. (3)**.

$$\Delta G_{criterion} = -\Delta G_{chem} - \left(\frac{x}{\bar{v}_{hyd}}\right)\left(\frac{\sigma_{\theta} \cos \phi}{3}\right)\bar{v}_H - \sigma_{\theta} \cos \phi \chi + \Delta G_{strain} \leq 0 \quad (3)$$

$$\sigma_{\theta, threshold} = \frac{-\Delta G_{chem} + \Delta G_{strain}}{\left(\frac{x}{\bar{v}_{hyd}}\right)\left(\frac{\cos \phi \bar{v}_H}{3}\right) + \cos \phi \chi} \quad (4)$$

W. Qin et al. assumed that all radial hydride precipitates at the prismatic plane with $\{10\bar{1}1\}_{\alpha-Zr} // \{111\}_{\delta-ZrH1.66}$ interface orientation relationship in the ideal texture of 100% radial basal pole [6]. However, the threshold hoop stress calculated with **Eq. (4)** from this assumption is 1885 MPa. It is markedly over-estimated when compared to the widely known range of threshold hoop stress obtained from mechanical experiments of many studies (65~138 MPa).

4. Results and discussion

The theoretically obtained threshold hoop stress can be more accurate, when realistic texture and Zr-hydride interface orientation relationship directly measured by EBSD with hydride reoriented specimens are reflected in prediction.

Realistic texture was identified from the basal plane pole figures of α -Zr. **Fig. 3(a)** shows both circumferential and radial hydrides, and **Fig. 3(b)** and **Fig. 3(c)** present pole figure of α -Zr in one of five areas containing radial hydrides and phase map of Zr-hydride. From the texture information of five radial hydride areas, the average angle of normal to basal plane from the radial direction ($\bar{\theta}$) is calculated to be 42.7° . Also, it is confirmed that the angle intensity of basal pole from the radial direction is the highest at 30° (see **Fig. 3(b)**). The average angle

of normal to basal plane from the radial direction ($\bar{\theta}$) will be used to calculate ϕ in **Eq. (3)** and **Table I** by using an equation $\phi = |\bar{\theta} + \psi - 90^\circ|$.

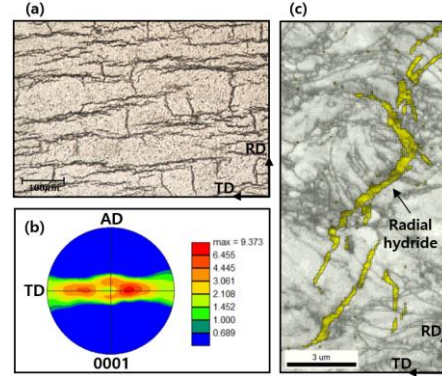


Fig. 3. (a) Optical microscopy of circumferential and radial hydrides; (b) Pole figure of α -Zr basal plane in hydride reoriented specimen; (c) Phase map of Zr-hydride (gray: α -Zr matrix, yellow: hydride)

Table I: The measured and calculated parameters on five radial hydride areas depending on five representative interface orientation relationship

Orientation Relationship	Plane relationship angle (ϕ)	Angle between hydride and hoop stress (ϕ)	Misfit strain (χ)	Strain energy (ΔG_{strain})	Average fraction (%)
$\{0001\}_{\alpha} // \{111\}_{\delta}$	$(0001) \perp (0001)$	47.3°	0.0520	$2.951 \times 10^8 \text{ J/m}^3$	49.37
$\{10\bar{1}7\}_{\alpha} // \{111\}_{\delta}$	$(0001) \perp (10\bar{1}7)$	32.6°	0.0537	$3.143 \times 10^8 \text{ J/m}^3$	4.41
$\{10\bar{1}3\}_{\alpha} // \{111\}_{\delta}$	$(0001) \perp (10\bar{1}3)$	15.7°	0.0590	$3.801 \times 10^8 \text{ J/m}^3$	4.92
$\{10\bar{1}1\}_{\alpha} // \{111\}_{\delta}$	$(0001) \perp (10\bar{1}1)$	14.2°	0.0717	$5.607 \times 10^8 \text{ J/m}^3$	36.81
$\{10\bar{1}0\}_{\alpha} // \{111\}_{\delta}$	$(0001) \perp (10\bar{1}0)$	42.7°	0.0775	$6.541 \times 10^8 \text{ J/m}^3$	4.49

According to five representative interface orientation relationships between α -Zr and δ -hydride [7], **Table I** shows the average fraction of orientation relationships from five radial hydride areas and values of many parameters to each orientation relationship. The dominant orientation relationship was the basal plane interface $\{0001\}_{\alpha-Zr} // \{111\}_{\delta-ZrH1.66}$ followed by the prismatic plane interface $\{10\bar{1}1\}_{\alpha-Zr} // \{111\}_{\delta-ZrH1.66}$. **Fig. 4** shows that the interface orientation relationship are mainly covered with blue and red lines that represent $\{0001\}_{\alpha-Zr} // \{111\}_{\delta-ZrH1.66}$ and $\{10\bar{1}1\}_{\alpha-Zr} // \{111\}_{\delta-ZrH1.66}$. It is now understandable with **Table I** that the threshold hoop stress with W. Qin's assumption is very high, because the strain energy at prismatic plane interface is the highest. If realistic values are used in calculation with **Eq. (4)** by reflecting the experimentally measured average fraction of each orientation relationship instead of the assumption, the accuracy of prediction for hydride reorientation threshold will be improved. The fraction-weighted average misfit strain and strain energy could represent the macroscopic radial hydride in Zr matrix. Accordingly, the fraction-weighted average misfit strain is calculated to be $\bar{\chi} = 0.06082$, and the corresponding average strain energy is $\overline{\Delta G}_{strain} = 4.1402 \times 10^8 \text{ J/m}^3$. Also, the fraction-weighted average angle ($\bar{\phi}$) is calculated to be 32.7° . From the prediction with these values in **Eq. (4)**, the updated threshold hoop stress for

hydride reorientation is 121 MPa which is located in the threshold range (65~138 MPa) as shown in Fig. 5 and more accurate compared to the previous over-estimated threshold stress, 1885 MPa. Therefore, it is proved that the reflection of fraction-weighted average parameters based on direct EBSD observation improves the accuracy of threshold stress prediction.

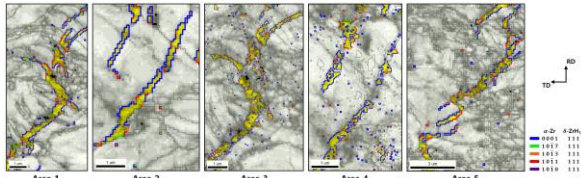


Fig. 4. Phase map of five radial hydride areas (Zircaloy-4 tubular specimen, ~458 wppm hydrogen concentration, 122 MPa hoop stress)

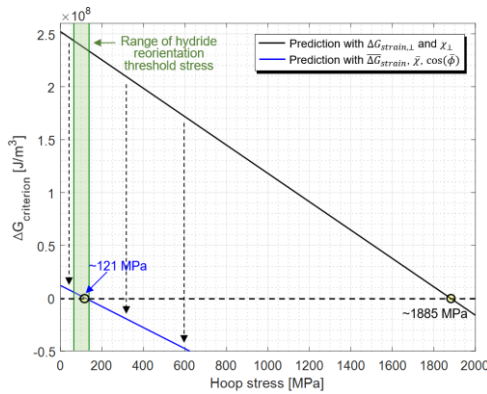


Fig. 5. Threshold hoop stress for hydride reorientation

As discussed above, the highest angle intensity in the pole figure of α -Zr basal plane is at 30° and the two dominant interface orientation relationships in radial hydrides are $\{0001\}_{\alpha\text{-Zr}} // \{111\}_{\delta\text{-ZrH1.66}}$ and $\{10\bar{1}1\}_{\alpha\text{-Zr}} // \{111\}_{\delta\text{-ZrH1.66}}$. It implies that the macroscopic radial hydrides in Zr matrix are primarily formed in a combination of two formation cases. In the first case, hydride platelets nucleate with $\{0001\}_{\alpha\text{-Zr}} // \{111\}_{\delta\text{-ZrH1.66}}$ orientation relationship (the first dominant orientation relationship) and interlink in radial direction on the basal planes of α -Zr whose normal to basal plane is perpendicular to the radial direction with low intensity in the pole figure as shown in Fig. 6(a). The number of available nucleation sites is limited because of the engineered texture of commercial Zircaloy-4 cladding tube. However, the orientation relationship in this case is energetically favored due to the lowest strain energy (see Table I). In the second case, radial hydrides form on the first-order pyramidal plane of α -Zr whose normal to basal plane is tilted by 30° from the radial direction with the highest intensity in the pole figure as shown in Fig. 6(b). Although the orientation relationship, $\{10\bar{1}1\}_{\alpha\text{-Zr}} // \{111\}_{\delta\text{-ZrH1.66}}$, is not energetically favorable in terms of strain energy, this orientation relationship is statistically favored because of the large number of nucleation sites. The typical macroscopic radial hydride resulted from hydride reorientation is formed upon an aggregation of

$\{0001\}_{\alpha\text{-Zr}} // \{111\}_{\delta\text{-ZrH1.66}}$ and $\{10\bar{1}1\}_{\alpha\text{-Zr}} // \{111\}_{\delta\text{-ZrH1.66}}$ orientation relationships in mesoscale, as illustrated in Fig. 6(c).

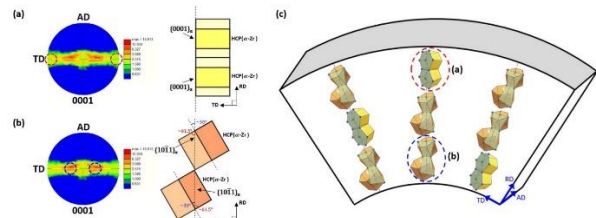


Fig. 6. Texture of α -Zr matrix and illustration of hydride nucleation habit plane for interface orientation relationships (a) $\{0001\}_{\alpha\text{-Zr}} // \{111\}_{\delta\text{-ZrH1.66}}$ and (b) $\{10\bar{1}1\}_{\alpha\text{-Zr}} // \{111\}_{\delta\text{-ZrH1.66}}$; (c) Schematic illustration of macroscopic radial hydrides consisting of the two dominant orientation relationships

5. Conclusions

Hydride reorientation was induced in Zircaloy-4 tubular specimens by means of mechanical experiment and the microstructure directly measured from tested specimens was analyzed in this study. The thermodynamic model to predict threshold hoop stress for hydride reorientation was further advanced in that the orientation relationship fraction-weighted misfit strain ($\bar{\chi}$) and strain energy ($\Delta\bar{G}_{strain}$) calculated by reflecting EBSD information replaced the existed misfit strain (χ) and strain energy (ΔG_{strain}) in the model. As a result, the accuracy of theoretically predicted threshold hoop stress progressed (from 1.885 GPa to 121 MPa) and the advanced threshold hoop stress, 121 MPa, agreed well with the range of threshold hoop stress from other experimental results. Furthermore, the formation of radial hydrides was illustrated in macroscopic level, based on the observed texture and dominant orientation relationships. This work allows us to understand and deal with hydride reorientation. Also, it is recommended to investigate other types of cladding materials as well for further studies.

ACKNOWLEDGEMENTS

This work was supported by the Nuclear Safety Research Program through the Korea Foundation Of Nuclear Safety (KoFONS) using the financial resource granted by the Nuclear Safety and Security Commission (NSSC) of the Republic of Korea [No.2003018]

REFERENCES

- [1] R.S. Daum, S. Majumdar, Y. Liu, M.C. Billone, J. Nucl. Sci. Technol. 43(9) (2006) 1054-1067.
- [2] A. Alam, C. Hellwig, Cladding tube deformation test for stress reorientation of hydrides, Zirconium in the Nuclear Industry: 15th International Symposium, ASTM International, 2009.
- [3] F. Nagase, T. Fuketa, J. Nucl. Sci. Technol. 41(12) (2004) 1211-1217.

- [4] J.J. Kearns, C.R. Woods, *J. Nucl. Mater.* 20(3) (1966) 241-261.
- [5] W. Qin, N.A.P. Kiran Kumar, J.A. Szpunar, J. Kozinski, *Acta Mater.* 59(18) (2011) 7010-7021.
- [6] W. Qin, J.A. Szpunar, J. Kozinski, *Acta Mater.* 60(12) (2012) 4845-4855.
- [7] J.A. Szpunar, W. Qin, H. Li, N.A.P. Kiran Kumar, *J. Nucl. Mater.* 427(1) (2012) 343-349.